Highly efficient organic optoelectronic conversion induced by electric double layers in ionic liquids

Cite as: Appl. Phys. Lett. **100**, 163304 (2012); https://doi.org/10.1063/1.3697988
Submitted: 18 January 2012 . Accepted: 06 March 2012 . Published Online: 19 April 2012

Bo Li, Yukiko Noda, Laigui Hu, Hirofumi Yoshikawa, Michio M. Matsushita, and Kunio Awaga

Highly efficient organic optoelectronic conversion induced by electric double layers in ionic liquids

Bo Li,[1,2,a)] Yukiko Noda,[1] Laigui Hu,[1,2] Hirofumi Yoshikawa,[1] Michio M. Matsushita,[1] and Kunio Awaga[1,3,b)]
[1]*Department of Chemistry and Research Center for Materials Science, Nagoya University, Nagoya 464-8602, Japan*
[2]*Department of Applied Physics, Zhejiang University of Technology, Hangzhou 310023, People's Republic of China*
[3]*CREST, JST, Nagoya 464-8602, Japan*

(Received 18 January 2012; accepted 6 March 2012; published online 19 April 2012)

In the present paper, highly efficient organic optoelectronic conversion has been demonstrated, induced by the electric double layers (EDLs) in ionic liquids. For the organic photocell, indium tin oxide/ionic liquid/charge-separation layer (zinc phthalocyanine:fullerene)/aluminum, in which the EDLs enhance the charge separation, a large photocurrent response can be generated. By this method, the internal quantum efficiency can reach 93% and a responsivity of 142 mA/W can be achieved. Since the EDLs show little dependence on the thickness of the ionic liquid, a very large photocurrent can be produced without the electrodes being superimposed along the light path. © *2012 American Institute of Physics*. [http://dx.doi.org/10.1063/1.3697988]

Electric double layers (EDLs) formed at ionic liquid/solid interfaces have received much attention because of their broad applications in electrochemistry, photochemistry, catalysis, energy storage, and electronics.[1] However, until now there has been no study on the application of EDLs to organic optoelectronic conversion. The Helmholtz model[2] indicates that, if an ionic liquid is inserted between an electrode and an organic semiconductor, the potential difference between them forms EDLs at the ionic liquid/solid interfaces, and potential drops are confined within the outer Helmholtz plane (OHP), as shown in Figure 1(a). It is also notable that the thickness of the OHP is nearly independent of the thickness of the electrolyte. This feature is very different from those of solid-state dielectric materials, in which the potential change occurs linearly (Figure 1(b)), so that the charge accumulation at their interfaces significantly depend on their thickness. The ultrathin potential drop region caused by the EDLs allows for high density charge accumulation,[3] which can be exploited for organic optoelectronic conversion.

To date, all the organic photocells possess one common structural feature, where a photoactive organic layer is sandwiched between two electrodes. One electrode is transparent for illumination, and through it the incident light excites the photoactive layer. The generated charges, after charge separation, are accumulated at the electrodes, producing a conduction current.[4] Due to the low carrier mobilities of organic semiconductors, the organic layer between the two electrodes should be thin, and only the superimposed area between top and bottom electrodes is available for photocurrent generation,[5] as shown in Figure 2(a). In general, there is no photocurrent contribution from illumination of the non-superimposed area because of a poor collection of the photocarriers, due to ohmic losses.[6] This type of organic photocell has many drawbacks, such as the difficulty in thin and large-area fabrication of the organic layer without pin holes, and the most critical point is the limitation of transparent electrode materials. Indium tin oxide (ITO) has been widely used as the most popular incident electrode due to its transparency,[7] but it is expensive and brittle.[8] Therefore, as shown in Figure 2(b), if direct excitation of the organic layer can effectively produce photocurrent between the two electrodes which are not superimposed along the light path, such electrode-position-free (EPF) photocurrent will renew the operation principle, the photocell design and the material innovation for organic photodetection, sensing, and optical communication, because transparency is no longer an indispensable condition for the electrodes.

To realize highly efficient EPF organic optoelectronic conversion, the present work is based on the idea of combining displacement current and ionic liquids, which has attracted much attention in electronics due to its potential applications in various devices, such as capacitors, batteries, solar cells, fuel cells, and actuators.[9] Recently, ionic liquids have been utilized as gate-dielectrics for organic thin film transistors (OTFTs),[10] because high-density carrier accumulation can be realized through the EDLs formed at the interface between the organic semiconductor and the ionic liquid. Displacement current is not an electric current of moving charges, but a time-varying change in electric field, to which

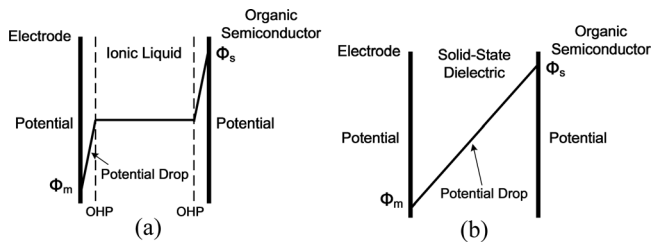

FIG. 1. Potential drops in ionic liquid (a) and solid-state (b) dielectrics, which are sandwiched by an electrode and organic semiconductor.

a)Electronic mail: libo@zjut.edu.cn.
b)Electronic mail: awaga@mbox.chem.nagoya-u.ac.jp.

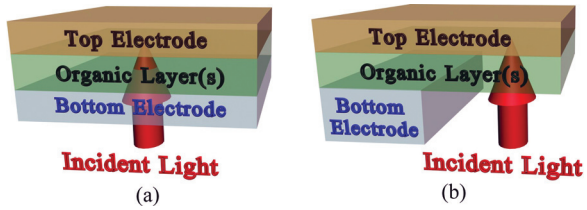

FIG. 2. (a) The structure of conventional organic photocells, in which the incident light irradiates the superimposed area between top and bottom electrodes. (b) The structure of electrode-position-free organic photocells, in which the incident light directly irradiates the organic layer(s) without passing through the bottom electrode.

dielectric polarizations in materials make a dominant contribution. Therefore, the propagation of displacement current does not need direct contact between an electrode and the photoactive layer,[11] whereas such direct contacts are critical for the conduction current in conventional organic photocells.[4–8]

To produce displacement current effectively, we have recently developed an organic photocell structure of electrode 1/polarization layer (PL)/charge-separation layer (CSL)/Electrode 2, where one of the electrodes is transparent. The insulating PL between the CSL and the electrode acts as a capacitor to induce the displacement current, and to propagate it from the CSL to the Electrode 2. When a capacitor is introduced into a circuit, the capacitive reactance should be considered. The relation between the capacitance C and the capacitive reactance X_C is

$$X_c = \frac{1}{2 \cdot \pi \cdot f \cdot C}, \tag{1}$$

where f is the frequency. The larger the capacitance, the smaller the capacitive reactance, resulting in an increase in the alternating current. In this context, ionic liquids are suitable candidates for PL because of their large capacitance caused by the formation of electric double layers (EDLs) at liquid/solid interfaces,[12] and high ionic conductivities.[13] Note that the EDLs depend little on the thickness of the ionic liquid, so that displacement current can be produced even if the two electrodes are separated by a long distance. When the EDLs have been introduced into the photocells, the present mechanism is not suitable for solar cells which produce steady-state current, but it is suitable for organic photodetection, sensing, and optical communication.

Two kinds of ITO/PL/CLS/Aluminum (Al) photocells were fabricated, in which an ionic liquid, *N*,*N*-diethyl-*N*-methyl(2-methoxyethyl) ammonium bis(trifluoromethylsulfonyl)imide (DEME-TFSI), and a well-known polymer dielectric, polyvinylidene fluoride (PVDF), were adopted as PL. The CSLs were common: a blend thin-film of zinc phthalocyanine (ZnPc) and fullerene (C_{60}) (ratio 1:1, 50 nm) fabricated by vacuum vapor deposition. The photocell structures are schematically shown in Figures 3(a) and 3(b), and the measurement diagram is illustrated in Figure S1.[14] The photocells were irradiated from the ITO side by a 532 nm continuous wave (CW) laser modulated by a light chopper at 3000 Hz, with an output power density of 13 mW/cm^2. The photocurrent was measured using a current amplifier and an oscilloscope without a bias voltage.

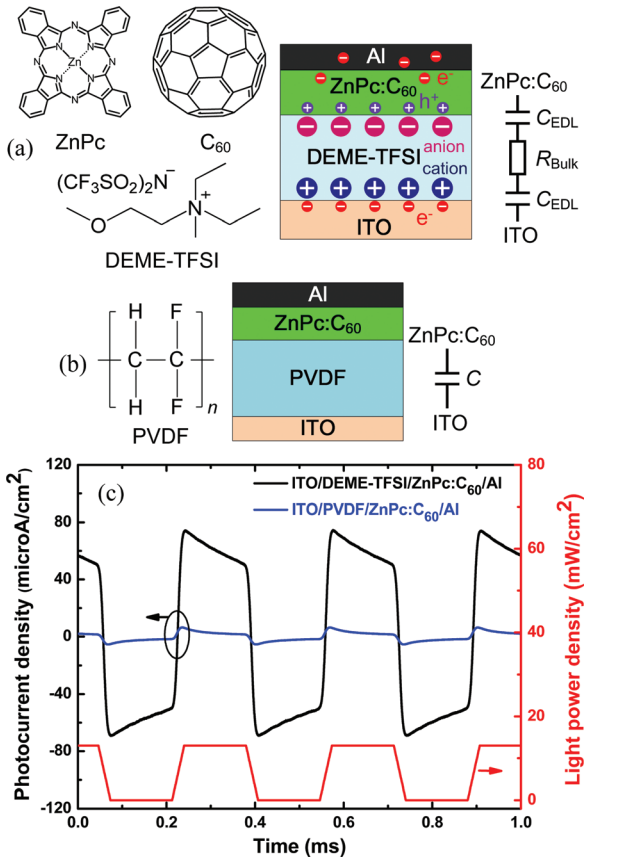

FIG. 3. (a) The device structure of ITO/DEME-TFSI/ZnPc:C_{60}/Al with the molecular structures of ZnPc, C_{60} and DEME-TFSI. The equivalent circuit is also shown, in which the two C_{EDL} are the capacitors formed at the interfaces, and the R_{Bulk} is the resistor of bulk DEME-TFSI. (b) The device structure of ITO/PVDF/ZnPc:C_{60}/Al, the molecular structure of PVDF, and the equivalent circuit, in which C is the capacitor for the PVDF layer. (c) The photoresponse of the ITO/DEME-TFSI (0.15 mm)/ZnPc:C_{60} (50 nm)/Al (black curve) and ITO/PVDF (200 nm)/ZnPc:C_{60} (50 nm)/Al (blue) photocells under illumination of a light-chopper-modulated 532 nm laser (3000 Hz) with a power density of 13 mW/cm^2. The red curve shows the time dependence of the incident light power density.

The red curve in Figure 3(c) shows the time dependence of the incident light power density, measured with a silicon photodiode. The black curve in Figure 3(c) shows the time trajectory of the photocurrent for the ITO/DEME-TFSI/ZnPc:C_{60}/Al cell. When the light turns on, the current quickly increases, and, after making a maximum, it shows a gradual decrease. When the light turns off, the current suddenly changes the polarization from positive to negative, and after passing through a negative peak, it shows a gradual decrease. The black curve clearly shows a very effective production of displacement current. The blue curve in this figure shows the photocurrent of the ITO/PVDF/ZnPc:C_{60}/Al cell. This curvature is similar to that of the black one, but the photocurrent of the PVDF cell is smaller than that of the DEME-TFSI cell by more than one order of magnitude, even though they have the common CSL. As is expected, the displacement current is significantly enhanced by the ionic-liquid PL.

We briefly discuss the mechanism of the transient current, following the discussion in reference.[15] Figure 3(b) includes the equivalent circuit of the ITO/PVDF/ZnPc:C_{60}/Al photocell. The modulated periodical light-on and -off produce an alternating electric field in the PL. During the light-on period, the field intensity increases, and the equivalent

capacitor is charged up, and, in the following light-off period, the negative transient photocurrent appears due to the discharging of the capacitor, decreasing the electric field intensity.

Figure 3(a) includes the equivalent circuit of the ITO/DEME-TFSI/ZnPc:C_{60}/Al photocell, in which the PL corresponds to the two capacitors and one resistor in between, due to the formation of EDLs at both the solid/liquid interfaces. Since, this C_{EDL}-R_{BULK}-C_{EDL} series can be regarded as a capacitor, however, we can apply the above discussion to this photocell. In fact, the device capacitance of the DEME-TFSI and PVDF cells were estimated as 18.3 nF and 0.5 nF at 3000 Hz, respectively. The capacitance of the former was much larger than that of the latter,[3,16,17] due to the formation of EDLs, which was reported to be maintained up to 100 kHz.[17] This is consistent with the extremely large transient photocurrent of the DEME-TFSI photocell.

The external quantum efficiency (EQE) and the internal quantum efficiency (IQE) were estimated for the ITO/DEME-TFSI/ZnPc:C_{60}/Al photocells. In these measurements, the thickness of the CSL was thin (25 nm) due to the low conductivity and the short exciton diffusion length (<50 nm) in the organic materials.[18] Figure 4(a) shows the wavelength dependence of the EQE and IQE, which were calculated from the peak values of the transient photocurrent during the light-on period. Their wavelength dependence agrees well with the absorption spectrum of the CSL shown in Figure 4(b). The peak value of the IQE reaches 93%, which indicates nearly all the absorbed photons have been converted into photocurrent. It is worth noting that the high density charge accumulation in the PL would enhance the charge separation in the CSL. Furthermore, the responsivity R_i of this photocell was calculated, using,

$$R_i = \frac{I_{ph}}{P_{opt}} = \frac{q \cdot \lambda \cdot EQE}{h \cdot c}, \quad (2)$$

where I_{ph} is the produced photocurrent, P_{opt} is the input light power, hc/λ is the photon energy, and q denotes the elementary charge. The responsivity at 620 nm without a bias voltage, corresponds to 142 mA/W, which is much larger than those of the conventional organic photodetectors operated by a bias voltage.[19]

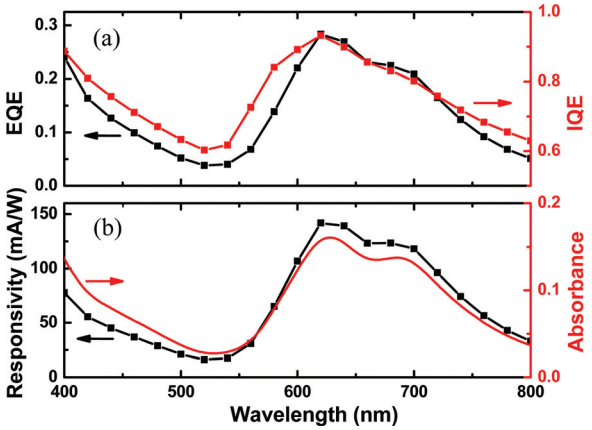

FIG. 4. (a) EQE (black line) and IQE (red line) spectra of the ITO/DEME-TFSI (0.15 mm)/ZnPc:C_{60} (25 nm)/Al photocells obtained by irradiation of the light-chopper-modulated monochromatic light from 400 nm to 800 nm (3000 Hz) without a bias voltage, which are calculated from the peak current of the photocells. (b) Responsivity spectrum (black), which is calculated from the EQE and the absorbance spectrum (red) of ZnPc:C_{60} (ratio 1:1, 25 nm) blend film.

The EPF measurements were carried out, with the ITO/DEME-TFSI (0.15 mm)/ZnPc:C_{60} (50 nm)/Al and ITO/PVDF (200 nm)/ZnPc:C_{60} (50 nm)/Al cells, in which the linear-patterned ITO and Al electrodes make a cross, sandwiching the CSL and PL (see Figure 5(a)). The widths of the ITO and Al electrodes are 2 and 1 mm, respectively. These photocells were illuminated from the ITO side under the same conditions described for Figure 3(c). The laser spot size diameter was 0.36 mm. The photocurrent was recorded, moving the illumination spot along the line-shape Al electrode from the superimposed to non-superimposed area, as shown in the Figure 5(a). When the illuminated spot in the CSL deviates from the cross-section area in the present photocell structure, there is an increase in the thickness of the PL between the ITO and the excited CSL area. Figure 5(b) shows the plots of the photocurrent (peak values in Figure S4[14]) vs. the distance d which represents the distance between the laser spot and the right edge of the ITO electrode. The photocurrent is normalized by the value obtained at $d = -1$ mm, the center of the crossing area. Although the

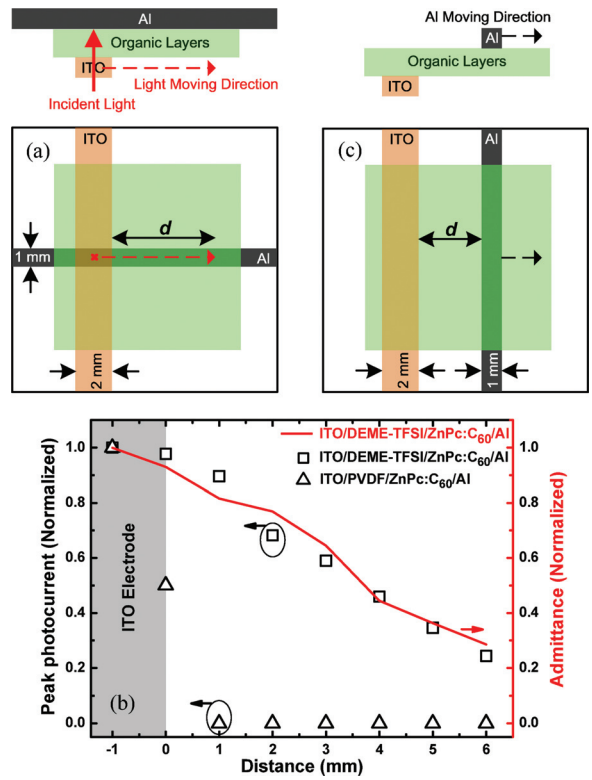

FIG. 5. (a) The scheme for the EPF measurements: cross section and bottom views, in which the incident light spot (red cross) moves from the center of the superimposed area between ITO and Al to the non-superimposed area along the line-shape Al electrode. (b) The distance dependence of the light-on peak photocurrent for the DEME-TFSI (square) and PVDF (triangle) photocells, and the values are normalized by those at $d = -1$ mm. The distance d is between the laser spot (0.36 mm in diameter) and the right edge of the ITO electrode (see (a)), and the red curve shows the admittance of the DEME-TFSI cell, in which the values are normalized by that at $d = -1$ mm. (c) The scheme for the cell impedance measurements: cross section and bottom views, in which the Al electrode is parallel to the ITO electrode and d represents the gap distance between the two electrodes.

PVDF cell exhibits no photocurrent from the non-superimposed area, the photocurrent of the DEME-TFSI cell shows only a gradual decrease with an increase in d. Surprisingly, the current is still more than 20% of the original value at a macroscopic distance of $d = 6$ mm, which is much larger than the thickness of the CSL.

Figure S3[14] shows the results for the ITO/poly(3,4-ethylenedioxythiophene):poly(styrenesulfonate) (PEDOT:PSS)/ZnPc:C_{60} (50 nm)/DEME-TFSI (0.15 mm)/Al cell, in which the CSL is separated from the Al electrode by DEME-TFSI. In this case, hole accumulation takes place at the ITO side. This photocell was also found to exhibit a large displacement current, and EPF properties.

The above phenomena indicate the universality of the EPF system, which means either the anode or cathode electrode position can be free. It is also clear that this property is caused by the formation of EDLs. When the illuminated spot in the CSL deviates from the cross-section area in the present photocell structure, there is an increase in the thickness of the PL between the ITO and the excited CSL area. Regarding solid-state PLs such as PVDF, the whole PL works as a uniform capacitor (see the equivalent circuit in Figure 3(b)). Therefore, the capacitive reactance of the PL shows a linear increase with an increase in its thickness; e.g., the capacitive reactance of PVDF of 1 mm thickness is larger than that of 200 nm by 5000 times. It is reasonable for the PVDF cells not to exhibit EPF photocurrent; the photocurrent at $d \geq 1$ mm is negligibly small, compared to that at $d = 0$ mm. Figure 3(a) shows the equivalent circuit of the DEME-TFSI cells, having a C_{EDL}-R_{BULK}-C_{EDL} structure. As is mentioned in the introduction, the C_{EDL} depend little on the thickness of the DEME-TFSI layer. Though R_{BULK} linearly increases with the layer thickness, the impedance of the whole cell only shows a small increase. For this reason, transient photocurrent of the DEME-TFSI cell is maintained.

The PL-thickness dependence of the impedance for the ITO/DEME-TFSI/ZnPc:C_{60}/Al cells was examined, using a measurement setup in Figure 5(c), where the line-shape of ITO and Al electrodes were parallel. The obtained admittances are plotted against the distance between ITO and Al as a red curve in Figure 5(b), in which their values are normalized by that at $d = -1$ mm. The red curve explains well the dependence of the photocurrent, indicating that the EPF property of the ionic-liquid photocells owes to the formation of EDLs.

In summary, we have obtained extremely large displacement current from the ITO/DEME-TFSI/ZnPc:C_{60}/Al photocells, due to the high density charge accumulation, caused by the formation of EDLs at the solid/liquid interfaces. The responsivity and IQE of these photocells reached 142 mA/W and 93%, respectively. Since the EDLs depended little on the thickness of the ionic liquid, the light-induced displacement current was effectively produced, even by illumination at the non-superimposed area between anode and cathode electrodes. Such EPF optoelectronic conversion can be used for photodetectors, sensors, and optical communication devices and should have great implications; any conducting materials can be used as the electrodes in organic optoelectronic devices, regardless of their transparency, and tandem cell structures can be easily fabricated for broad light-harvesting bands.

This research was supported by a Grant-in-Aid for Scientific Research from the Ministry of Education, Culture, Sports, Science, and Technology (MEXT) of Japan. The authors wish to thank Dr. Simon Dalgleish for valuable discussions and helpful comments on this manuscript. Dr. Li also thanks the National Science Foundation of China (No. 61008008).

[1]J. H. Cho, J. Lee, Y. Xia, B. Kim, Y. He, M. J. Renn, T. P. Lodge, and C. D. Frisbie, Nature Mater. **7**, 900 (2008); A. S. Dhoot, C. Israel, X. Moya, N. D. Mathur, and R. H. Friend, Phys. Rev. Lett. **102**, 136402 (2009); J. T. Ye, S. Inoue, K. Kobayashi, Y. Kasahara, H. T. Yuan, H. Shimotani, and Y. Iwasa, Nature Mater. **9**, 125 (2010).
[2]H. von Helmholtz, Ann. Phys. Chem. **243**(7), 337 (1879); H. Wang and L. Pilon, J. Phys. Chem. C **115**, 16711 (2011).
[3]H. Yuan, H. Shimotani, A. Tsukazaki, A. Ohtomo, M. Kawasaki, and Y. Iwasa, Adv. Funct. Mater. **19**, 1046 (2009).
[4]B. C. Thompson and J. M. J. Fréchet, Angew. Chem., Int. Ed. **47**, 58 (2008); K. M. Coakley and M. D. McGehee, Chem. Mater. **16**, 4533 (2004).
[5]X. Gong, M. Tong, Y. Xia, W. Cai, S. M. Ji, Y. Cao, G. Yu, C. L. Shieh, B. Nilsson, and A. J. Heeger, Science **325**, 1665 (2009); T. M. Clarke and J. R. Durrant, Chem. Rev. **110**, 6736 (2010); C. J. Brabec, N. S. Sariciftci, and J. C. Hummelen, Adv. Funct. Mater. **11**, 15 (2001).
[6]G. Horowitz, Adv. Mater. **2**, 287 (1990).
[7]S. Günes, H. Neugebauer, and N. S. Sariciftci, Chem. Rev. **107**, 1324 (2007).
[8]Y. H. Kim, C. Sachse, M. L. Machala, C. May, L. Müller-Meskamp, and K. Leo, Adv. Funct. Mater. **21**, 1076 (2011).
[9]M. Armand, F. Endres, D. R. MacFarlane, H. Ohno, and B. Scrosati, Nature Mater. **8**, 621 (2009); P. Wang, S. M. Zakeeruddin, R. Humphry-Baker, and M. Grätzel, Chem. Mater, **16**, 2694 (2004); D.Kuang, P.Wang, S.Ito, S. M.Zakeeruddin, and M.Grätzel, J. Am. Chem. Soc. **128**, 7732 (2006).
[10]Y. Xia, J. H. Cho, J. Lee, P. P. Ruden, and C. D. Frisbie, Adv. Mater. **21**, 2174 (2009).
[11]A. Mohite, S. Chakraborty, P. Gopinath, G. U. Sumanasekera, and B. W. Alphenaar, Appl. Phys. Lett. **86**, 061114 (2005); T. Fukuma, K. Umeda, K. Kobayashi, H. Yamada, and K. Matsushige, Jpn. J. Appl. Phys. **41**, 4903 (2002).
[12]B. Skinner, T. Chen, M. S. Loth, and B. I. Shklovskii, Phys. Rev. E **83**, 056102 (2011); C. Largeot, C. Portet, J. Chmiola, P. L. Taberna, Y. Gogotsi, and P. Simon, J. Am. Chem. Soc. **130**, 2730 (2008); H. Itoi, H. Nishihara, T. Kogure, and T. Kyotani, *ibid.* **133**, 1165 (2011); M. V. Fedorov and A. A. Kornyshev, J. Phys. Chem. B **112**, 11868 (2008).
[13]R. Misra, M. McCarthy, and A. F. Hebard, Appl. Phys. Lett. **90**, 052905 (2007).
[14]See supplementary material at http://dx.doi.org/10.1063/1.3697988 for device fabrication, characterization, experimental setup, and photocurrent response.
[15]L. Hu, Y. Noda, H. Ito, H. Kishida, A. Nakamura, and K. Awaga, Appl. Phys. Lett. **96**, 243303 (2010).
[16]H. Yuan, H. Shimotani, A. Tsukazaki, A. Ohtomo, M. Kawasaki, and Y. Iwasa, J. Am. Chem. Soc. **132**, 6672 (2010).
[17]H. Yuan, H. Shimotani, J. Ye, S. Yoon, H. Aliah, A. Tsukazaki, M. Kawasaki, and Y. Iwasa, J. Am. Chem. Soc. **132**, 18402 (2010).
[18]P. Peumans, A. Yakimov, and S. R. Forrest, J. Appl. Phys. **93**, 3693 (2003); L. G. Yang, H. Z. Chen, and M. Wang, Thin Solid Films **516**, 7701 (2008).
[19]A. Iwasaki, L. Hu, R. Suizu, K. Nomura, H. Yoshikawa, K. Awaga, Y. Noda, K. Kanai, Y. Ouchi, K. Seki, and H. Ito, Angew. Chem., Int. Ed. **48**, 4022 (2009); K. S. Narayan and T. B. Singh, Appl. Phys. Lett. **74**, 3456 (1999); G. A. O'Brien, A. J. Quinn, D. A. Tanner, and G. Redmond, Adv. Mater. **18**, 2379 (2006).